

Early Stages of Zinc Corrosion and Runoff Process Induced by Caribbean Sea Water

E. Mena¹, L. Veleva^{1,*}, R. M. Souto²

¹Department of Applied Physics, Research Center for Advanced Study (CINVESTAV-IPN), Mérida Carr. Ant. a Progreso Km. 6, 97310, Mérida, Yucatán, México

²Department of Chemistry, University of La Laguna, 38071 La Laguna, Tenerife, Canary Islands, Spain

*E-mail: veleva@mda.cinvestav.mx

Received: 16 June 2015 / Accepted: 8 July 2015 / Published: 28 July 2015

Flat samples of electrolytic zinc were immersed for periods of 8, 10, 30 and 90 days in Caribbean Sea water for further analysis of the corrosion behavior and runoff process using different techniques. The free corrosion potential (o.c.p.) were monitored and correlated with the runoff rate. The Zn^{2+} ions released from anodic sites interact with the OH^- ions formed at the cathodic sites, giving origin to the slightly soluble $Zn(OH)_2$ precipitated during the experiment. X-ray diffraction analysis revealed the formation of several zinc hydroxides. The main corrosion product was *simonkolleite* [$Zn_5(OH)_8Cl_2 \cdot H_2O$], and as minority phases two *zinc carbonate hydroxides*, [$Zn_5(CO_3)_2(OH)_6$] and [$Zn_4CO_3(OH)_6 \cdot H_2O$], and later stages $Mg_9Zn_4(SO_4)_2(OH)_{22} \cdot 8H_2O$ and $Zn(OH)_2$. The changes of pH in the interface zinc/substitute ocean water were monitored *in situ* with scanning electrochemical microscopy (SECM) technique and the local anodic and cathodic sites were mapped. Due to the corrosion reaction, the initial pH of sea water was diminished to 4.4 at the anodic sites as a consequence of metal ion hydrolysis. This fact led to the formation of a complex variety of zinc corrosion products, consuming at least a fraction of the produced OH^- ions.

Keywords: zinc, corrosion potential, sea water, runoff, SECM.

1. INTRODUCTION

Zinc is a component of the earth's crust and an inherent part of our environment. About 12 million tons of zinc are produced annually worldwide and half of this amount is used for galvanizing to protect steel from corrosion, due to its standard redox potential (-0.76 V / SHE) that is more negative than that of steel (-0.44 V / SHE). Zinc, particularly as hot dip galvanized steel, is a common metal for

corrosion protection of steel structures: laminated roofs, fences, containers and tubes for water transport, zinc sacrificial anodes for cathodic protection, zinc-rich coatings, etc. [1-4]. It is well known, from a thermodynamic point of view, that zinc is relatively stable in neutral and near neutral aqueous environments [5]. Initially a fresh zinc surface corrodes fairly rapidly until it is covered with corrosion product layers (zinc oxide/hydroxides/carbonates), which then act as a physical barrier between the metal and the aggressive environment, and the corrosion then continues at a reduced rate [6-8]. However, this so formed rust layer can be transformed into a nonprotective layer due either to physical removal of the layer (under the action of wind, flows and sand erosion) or from partial dissolution of some soluble corrosion products. As result, metal ions can be released from the metal surface to the surrounding environment. This phenomenon is recognized today as a metal runoff.

All life on earth has evolved in the presence of natural levels of zinc. Due to its general availability to organisms and unique characteristics, zinc has an essential role in various biological processes. As such, zinc is an essential element for all forms of life, from the smallest micro-organisms to man. The zinc industry has supported numerous studies in aquatic, terrestrial and atmospheric systems to further understanding of the natural variations of zinc in the environment. Consideration of background zinc concentrations has assisted environmental risk, providing a context for biological acclimation and adaptation [9]. Yet a high ionic zinc ion concentration in water can cause a toxic effect for aquatic life, for example [10]. The analysis of the literature shows that attention to the metal corrosion (in sea water) [11-13] and runoff is enormous in Europe and USA since 1990 [14-17]. Our previous studies have been focused in monitoring zinc runoff and changes that occur on the metal surface during the corrosion process in urban, rural and marine coastal environments [18-21].

Since zinc behaviour in sea water is an increasing topic of study, the generation of new data is of interest to the international environmental scientists and civil engineering community. This work presents the early stages of zinc runoff phenomenon in Caribbean sea water due to zinc corrosion during 8, 10, 30 and 90 days. The analysis was carried out with a systematic study of the free corrosion potential (at o.c.p.) fluctuations and runoff rate. The tendency of their changes were correlated with the corrosion products formed on zinc samples by using scanning electron microscopy (SEM) and X-ray diffraction (XRD) techniques, to assess the composition and morphology of these products. The pH distribution at the interface zinc/sea water was carried out *in situ* with scanning electrochemical microscopy (SECM) technique, since the initial immersion of zinc sample (electrode). Local changes of pH were used for identification of cathodic and anodic sites during the first stages of zinc corrosion in sea water. The results obtained from each approach were correlated. To our knowledge, no other research has been undertaken to date on this aspect.

2. EXPERIMENTAL

2.1. Zinc exposure and characterization

Electrolytic zinc flat samples (99.99 mass %; dimensions of 20 mm x 20 mm x 1.5 mm), three replicates were previously degreased with ethanol and immersed separately, each one in 65 mL of

Caribbean seawater at 21°C, in plastic containers for 8, 10, 30 and 90 days. Samples of zinc, withdrawn at these periods of exposure in seawater, were dried at room temperature and analyzed using various techniques. The crystalline corrosion products were characterized by X-Ray Diffraction Technique (XRD, Siemens D-5000, with grazing beam geometry, 3° angle, 34 kV / 25 mA and $\text{Cu}_{\text{K}\alpha}$ radiation). The spectra were processed with DIFRACT AT [22] software and the identification of the phases with Powder Diffraction File [23]. Scanning electron microscopes (SEM-EDS, Philips and XL-30 ESEM JEOL JSM-7600F) were used to obtain images of the surface morphology of zinc samples after their exposure to seawater.

The zinc ions (Zn^{2+}) released (runoff) from the sample surfaces after each period of exposure was determined with a Multiparameter Ion Specific Meter (Model HI 83200, Hanna Instruments). The lower and higher detection limits for zinc ions in aqueous solutions are 0.00 and 3.00 mg L⁻¹, respectively.

Single zinc samples were used as working electrode for immersion in seawater, inside an electrochemical cell. The changes in the free corrosion potential (E_{corr}) values were measured at the open circuit potential, o.c.p. (i.e., without imposed polarization of the sample) during 12,600 s (3.5 h), after various periods of exposure in seawater. A potentiostat/galvanostat computerized series G750 (Gamry instruments, Inc., Software PHE 200) was employed for the measurement of E_{corr} . The electrochemical set-up was completed using a calomel electrode (SCE, $E_{\text{Hg}^{2+}/\text{Hg}/\text{sat. KCl}} = 0.244$ V/SHE) as the reference, and a platinum plate as auxiliary electrode.

In order to study the local pH changes at the interface zinc/electrolyte *in situ*, substitute ocean water was used, that was prepared according to International Standard [24]. In this way, the specific sea contaminants and changes of environmental parameters (pH, temperature, flow rate, sea waves, pressure, calcareous deposit, salinity and biofouling) are avoided and the obtained results can be compared with those reported by another researchers. High-resolution SECM equipment, supplied by Sensolytics (Bochum, Germany), was employed for the spatially-resolved characterization of the local pH changes occurring at the zinc/seawater interface. The instrument was built around a PalmSens (Utrecht, The Netherlands) electrochemical interface, and precise positioning unit, all controlled with a personal computer. The zinc sample working electrode (4.3 mm x 1.3 mm) was mounted horizontally facing upward at the bottom of a electrochemical cell, submerged in 3.5 mL of substitute ocean water (pH = 8.3), and tested at open circuit potential, using an Ag/AgCl/(3 M) KCl reference electrode. Disc-shaped tip (micro-electrode) made of antimony, coated by its metal oxide, and surrounded by glass micropipette, was a sensitive pH sensor. The antimony microelectrode had 40- μm -diameter active surface. In order to quantify the localized pH distribution, the antimony oxide tip was calibrated from the measurement of the potential response transients towards pH change of the solution, using a sequence of eight buffer solutions covering the $4 \leq \text{pH} \leq 11$ range. Positioning of the antimony tip close to the surface was assisted with a video camera. A homemade voltage follower based on a 10^{12} Ω input impedance operational amplifier was connected between the electrochemical cell and the potentiometric input of the system [25-27]. Scan maps and 2D images of pH changes were obtained by scanning the tip parallel to the sample surface, at 30 μm constant height operation. SECM images were recorded rastering an area away from the sample edges (1000 μm x 4000 μm), using a scan rate of 50 $\mu\text{m s}^{-1}$. The data were plotted using Quickgrid software.

2.2. Seawater chemistry

Seawater is a very aggressive medium for the metals and can cause severe damage to metallic structures in a very short length of time. Usually this water contains the ions (in decreasing quantities) of Cl^- , Na^+ , SO_4^{2-} , Mg^{2+} , Ca^{2+} , K^+ , HCO_3^- , Br^- , B^{3+} , Sr^{2+} , F^- , and dissolved gases, such as O_2 y CO_2 [28]. The seawater was taken from the Caribbean Sea at the warm humid tropical climate marine test station of CINVESTAV-Merida (Telchac port, Yucatan Peninsula, Mexico $21^\circ 7' \text{ N}$, $89^\circ 25' \text{ W}$), at a depth of 10 m and a distance of 10 km from the coast. Rack stands holding zinc samples were submerged at that location for metal corrosion testing in marine environment. The seawater had total salinity of 37.48%, $\text{pH} = 7.69$, dissolved oxygen 1.1 ppm, and temperature of 21°C at that depth. Specific sea pollutants were (expressed in $\mu\text{M L}^{-1}$): 1.75 ammonium; 2.61 silicates; 0.28 phosphates; 0.04 nitrites, and 1.84 nitrates.

3. RESULTS AND DISCUSSION

3.1. Corrosion potential evolution and zinc runoff

Initially the free corrosion potential (o.c.p.) had value of -1.108 V (vs SCE) and at the end of the experiment (90 days), it shifted to less negative (-1.028 V). Figure 1 presents the free corrosion potential (o.c.p) fluctuations of zinc sample (electrode) after 8 and 90 days immersed in sea water. The zinc ion release (runoff) was detected at 8 days and Table 1 presents the values of zinc runoff rates determined at different periods of exposure in Caribbean seawater and the corresponding E_{corr} values.

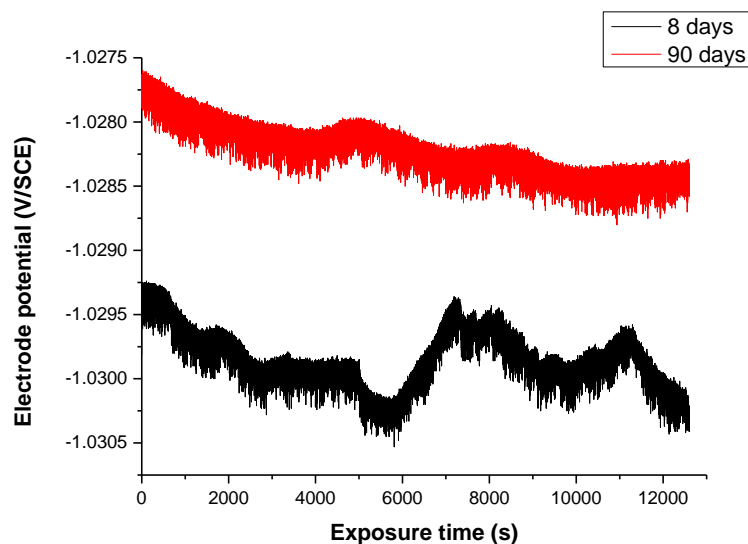


Figure 1. Electrode potential at o.c.p. after 8 and 90 days of exposure in Caribbean sea water.

The results (Table 1) showed that runoff rate of zinc ions increases from 3.20 g m^{-2} (at 8 days) up to 4.80 g m^{-2} at 30 days, when E_{corr} reached the most negative potential (increase of corrosion)

during the exposure test. After that period, runoff decreased to 4.50 g m⁻² (90 days), as a response of more noble value of E_{corr} . The observed relation between E_{corr} and zinc ion release should be correlated with the changes which occurred on the zinc surface.

Table 1. Zinc runoff rate and E_{corr} (o.c.p) values in Caribbean seawater.

Period (days)	Zinc (II) ions (mg L ⁻¹)	Runoff rate (g m ⁻²)	E_{corr} (V / SCE)
0	-	-	-1.108 / -1.094
8	1.92	3.20	-1.029 / -1.030
10	2.67	4.45	-1.091 / -1.047
30	2.90	4.80	-1.115 / -1.054
90	2.70	4.50	-1.027 / -1.028

In sea water, hydroxyl ions formed at all cathodic sites, as a consequence of reduction of the dissolved oxygen in seawater (equation 1), combine with zinc ions released (*runoff*) during the corrosion of the metal (equation 2) and they could produce different zinc hydroxides.



A white solid precipitation was observed on the bottom of the containers, at all stages of exposure of zinc samples. X-ray diffraction analysis revealed that the composition of the solid precipitate was mainly Zn(OH)₂, indicating that this product was removable from the zinc surface. Additional salts, corresponding to saline components of the seawater (NaCl, CaCO₃, CaSO₄, AlSiO₄ and SiO₂) were also present. However, according to the literature [29] zinc hydroxide is slightly soluble in water ($K_{sp} = 3 \times 10^{-17}$), supplying a route for the release (*runoff*) of free zinc ions in the seawater:



According to the computer model of zinc runoff made for Karlén et al, 2001 [30], zinc speciation (corrosion products) is a function of the pH of the water solution. The model predicts 95-99.9% of the released zinc to be present as free Zn(II) ions when the pH is acidic. Conversely, in neutral and alkaline electrolytes, the formation of Zn(OH)₂ and zinc carbonate corrosion products are favoured.

3.2. Analysis of surface zinc corrosion product

The corrosion potential changes and zinc runoff rate were correlated with the composition of the formed corrosion products, provided by X-ray diffraction (XRD). Table 2 presents a resume of the crystalline phases formed on the zinc surface, after each period of exposure in Caribbean seawater. Zinc surface morphology was characterized by scanning electron microscopy (SEM).

Table 2. Zinc corrosion products formed in Caribbean seawater

Period (days)	Zn crystalline phases	Seawater salts
8	Zn ₅ (OH) ₈ Cl ₂ .H ₂ O Zn ₅ (CO ₃) ₂ (OH) ₆ Zn ₄ CO ₃ (OH) ₆ .H ₂ O	NaCl CaCO ₃
10	Zn ₅ (OH) ₈ Cl ₂ .H ₂ O Zn ₄ CO ₃ (OH) ₆ .H ₂ O	NaCl CaCO ₃
30	Zn ₅ (OH) ₈ Cl ₂ .H ₂ O Mg ₉ Zn ₄ (SO ₄) ₂ (OH) ₂₂ . 8H ₂ O	NaCl
90	Zn ₅ (OH) ₈ Cl ₂ .H ₂ O Zn(OH) ₂	Ca ₈ Si ₁₆ O ₄₀ .11H ₂ O

It can be seen that after 8 days of exposure, on the zinc surface were formed three corrosion products and crystals of two seawater salts (Fig. 2, Fig. 3a,b). Thus, the formed layer was acting as a physical barrier between the metal and seawater, giving the shift of E_{corr} to more positive value (Table 1). However, after 10 days the sizeable crystals of carbonate were disappearing gradually, contributing to more accelerated attack on the zinc surface. As a result E_{corr} reached more negative values (Table 1). The main corrosion product of zinc was *simonkolleite* [Zn₅(OH)₈Cl₂.H₂O] in all periods of exposure, and the relative intensity of its peak in the diffractogram increased with time, reaching the maximum value at the end of this experiment (Fig. 2), when E_{corr} returned to less negative potential. So formed corrosion layer and the new seawater salt Ca₈Si₁₆O₄₀.11H₂O deposited on the zinc surface at 90 days (Table 1), could provide a better physical barrier against the acceleration of the corrosion process. As secondary minority corrosion phases were observed several zinc hydroxides: *hydrozincite* [Zn₅(CO₃)₂(OH)₆], *zinc carbonate hydroxide hydrate* [Zn₄CO₃(OH)₆.H₂O] and *torreyite* [Mg₉Zn₄(SO₄)₂(OH)₂₂.8H₂O]. The minority corrosion phase of *zinc hydroxide* [Zn(OH)₂] was detected on the metal surface only at the end of the experiment (i.e., 90 days, cf. Fig. 2). It was mentioned before that this product is considered to be the origin of free zinc ion release (runoff) in seawater. Zinc surface morphology at this period of time is presented in Figure 3 c,d.

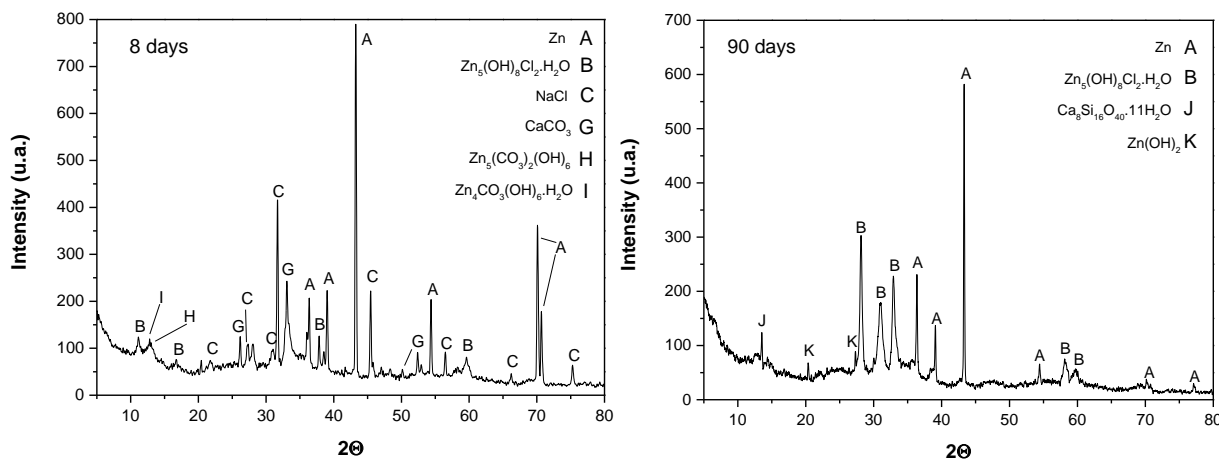


Figure 2. Diffraction patterns of the crystalline products deposited on the zinc surface after 8 (left) and 90 days (3 months, right) of exposure to Caribbean seawater.

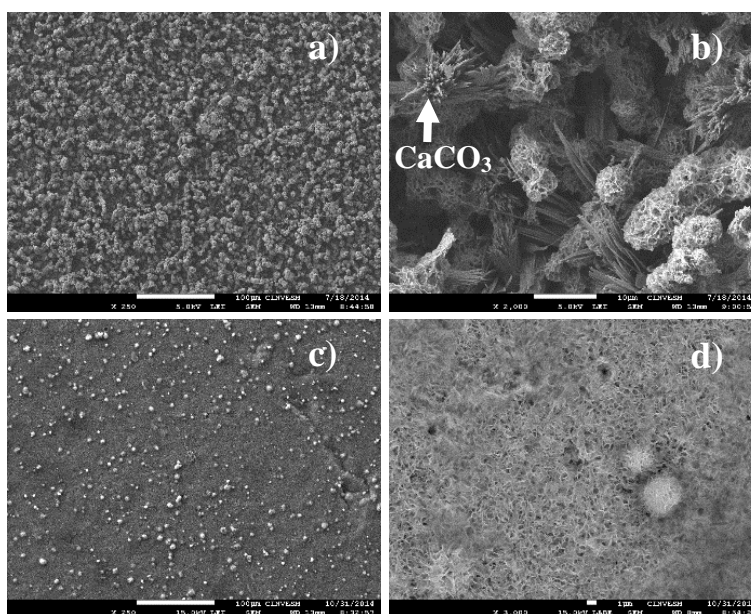


Figure 3. SEM photographs showing the corrosion layer of zinc surface after 8 (a, b) and 90 days (c, d) exposure to Caribbean seawater.

3.3. Local pH distribution at the zinc surface

Figure 4 shows the changes of pH at the interphase zinc/seawater during one hour of immersion in substitute ocean water. It can be seen that pH showed a variation in the range between 4.4 and 7.6. Due to cathodic and anodic reactions, which occur on the zinc surface, the initial pH = 8.3 of seawater was diminished. As it was mentioned before, OH⁻ ions are formed at the cathodic sites (Eq. 1) and pH should increase. However, the X-ray analysis revealed the formation of several zinc hydroxide corrosion products on the metal surface, consuming OH⁻ ions produced at the cathodic sites. Moreover, the OH⁻ ions are also captured by the Zn²⁺ ions released (runoff) at the anodic sites and this led to

the formation of the precipitated $\text{Zn}(\text{OH})_2$ reported in this study. The recorded pH map showed that the distribution of anodic and cathodic sites has a localized nature during zinc corrosion process (Fig. 4).

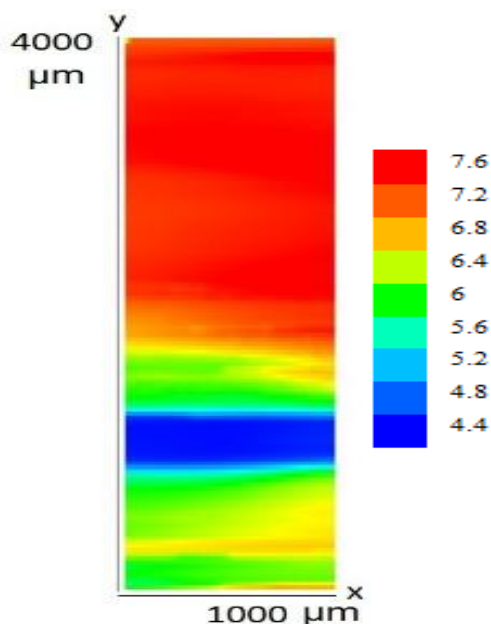


Figure 4. 2D pH distribution map recorded on the zinc surface after immersion in substitute ocean water during one hour. Scan dimensions: 1000 μm x 4000 μm .

It has been reported that, under tip polarization, zinc anodic sites are highly localized on the metal surface, originating corrosion pits [31], leading to local acidification as result of the hydrolysis of the metal ions formed in equation (2) as it follows:



The remaining exposed surface of the metal is available for the reduction of oxygen, effectively acting as a big cathode that releases OH^- ions. Yet, a neutral or alkaline local environment is only observed at locations on the surface sufficiently far from the active anode (i.e., the upper half of the pH distribution image). At locations closer to the active anodic region, the OH^- ions are partly neutralized by the protons released in metal hydrolysis, and mostly combine with soluble metal ions to form precipitated corrosion products. In this way, an almost symmetrical pH distribution is observed in the lower half of the image, centered around the anodic region. In resume, pH values changes, following the corrosion mechanism process, as a consequence of the variety of zinc layers formed at the metal/seawater interface around the anodic sites. It can also be noticed that corrosion product precipitation eventually may block the local anodic and cathodic sites, and the corrosion reactions shift to other locations on the surface progressively, eventually leading to the appearance of a quasi-homogeneous corrosion type [32], as already observed in the SEM micrographs given in Figure 3 that were obtained at longer exposures.

4. CONCLUSIONS

The aim of this study has been to provide information on the zinc corrosion behaviour in Caribbean Sea water at the early stages (8, 10, 30 and 90 days). During the period of test zinc ion release (runoff) was monitored and its changes were correlated with the free corrosion potential (E_{corr} at o.c.p.) fluctuations. The distribution of local pH changes at the zinc/sea water interface gave the possibility to map the location of cathodic and anodic sites. The results obtained and the analysis of the corrosion products formed on the zinc samples surface were discussed. The main conclusions are as following:

- The initial free corrosion potential (o.c.p.) had value of -1.108 V (vs SCE) and at the end of the experiment (90 days), it shifted to less negative (-1.028 V). The zinc ion release (runoff) was detected after 8 days of immersion in sea water and it reached the maximum rate of 4.80 g m^{-2} , corresponding to the most negative value of E_{corr} (-1.115 V). The tendency of E_{corr} matches well with the runoff rate changes.

- White solid precipitation was observed at the bottom of the containers, indicating that this product was removable from the zinc surface. X-ray diffraction analysis revealed that its composition is $\text{Zn}(\text{OH})_2$. Due to its slightly solubility in water zinc hydroxide gives the origin of free zinc ions. This fact allows to consider that zinc ions release are part of the $\text{Zn}(\text{OH})_2$ corrosion product.

- X-ray diffraction analysis revealed the formation of several zinc hydroxides. The main corrosion product of zinc was *simonkolleite* [$\text{Zn}_5(\text{OH})_8\text{Cl}_2 \cdot \text{H}_2\text{O}$] after each period of exposure in seawater, which relative intensity increased in time. As secondary minority corrosion phases appeared two *zinc carbonate hydroxides* [$\text{Zn}_5(\text{CO}_3)_2(\text{OH})_6$] and [$\text{Zn}_4\text{CO}_3(\text{OH})_6 \cdot \text{H}_2\text{O}$], *sulfate hydroxide* [$\text{Mg}_9\text{Zn}_4(\text{SO}_4)_2(\text{OH})_{22} \cdot 8\text{H}_2\text{O}$] and $\text{Zn}(\text{OH})_2$.

- The changes of local pH (4.4 up to 7.6) at the interface zinc/substitute ocean water were monitored *in situ* using the SECM technique in potentiometric operation, and the local anodic and cathodic sites were mapped. Due to localized cathodic and anodic reactions, the initial pH of seawater (8.3) was diminished. The OH^- ions produced at the cathodic sites were consumed by the Zn^{2+} ions formed in the anodic reaction, giving the origin of hydroxide corrosion products, and as consequence the pH decreased. Moreover, the OH^- ions were also captured by the Zn^{2+} ions released (runoff) at the anodic sites and this led to the formation of the precipitated $\text{Zn}(\text{OH})_2$.

ACKNOWLEDGEMENTS

The authors gratefully acknowledge partial financial support of this study from CONACYT (Grant 179110). Emmanuel Mena wishes to thank CONACYT for the scholarship granted to him for his Master's study and for the visit in ULL, Tenerife, Spain (Department of Chemistry). The authors are indebted to MSci Dora Huerta for assistant in SEM-EDS acquisition images and to MSci Daniel Aguilar in XRD analysis. R.M. Souto acknowledges support by the Spanish Ministry of Economy and Competitiveness (MINECO, Madrid) and the European Regional Development Fund, under grant CTQ2012-36787.

References

1. S. Cramer, J. P. Carter, P. J. Linstrom, D. R. Flinn, Degradation of Metals in the Atmosphere. In: *Atmospheric Factors Affecting Corrosion of Zinc, Galvanized Steel and Copper*, S. W. Dean, T. S.

- Lee, editors. ASTM STP 965. Philadelphia: American Society for Testing and Materials, (1988)
2. C. J. Slunder, W. K. Boyd, *Zinc: Its Corrosion Resistance*, International Lead Zinc Research Organization (ILZRO), New York (1983).
 3. L. Veleva, R. Kane, Atmospheric corrosion. In: *Corrosion, Fundamentals, Testing and Applications*, S. D. Cramer and B. S. Covino Jr., editors, Metal Park, OH: ASM Handbook Series, ASM International, (2003).
 4. X. G. Zhang, *Corrosion and Electrochemistry of Zinc*, New York: Plenum, (1996).
 5. M. Pourbaix, *Atlas of Electrochemical Equilibria in Aqueous Solutions*. Houston, TX: NACE International-Cebelcor, (1974).
 6. J. M. Costa, J. Vilarrasa, *Br. Corros. J.*, 28 (1993) 117.
 7. T. E. Graedel, *J. Electrochem. Soc.*, 136 (1989) 193C.
 8. R. A. Legault, V. P. Pearson, *Atmospheric Factors Affecting the Corrosion of Engineering Metals*, ASTM STP 646, S. K. Coburn, editor, West Conshohocken. PA: ASTM International, (1978).
 9. IZA, *Zinc, a Sustainable Material*, Durham, NC: International Zinc Association, (2015). (http://www.zinc.org/about/sustainable_development_publications).
 10. L. Veleva, E. Meraz, M. Acosta, *Mater. Corros.*, 58 (2007) 348.
 11. B. M. Durodola, J. A. O. Olugbuyiro, S. A. Moshood, O. S. Fayomi, A. P. I. Popoola, *Int. J. Electrochem. Sci.*, 6 (2011) 5605.
 12. J. Zhang, C. Sun, Z. Yu, J. Cheng, W. Li, J. Duan, *Int. J. Electrochem. Sci.* 9 (2014) 5712.
 13. Z. Yu, J. Zhang, X. Zhao, Xia Zhao, J. Duan, X. Song, *Int. J. Electrochem. Sci.*, 9 (2014) 7587
 14. J. W. Spence, F. H. Haynie, F. W. Lipfert, S. D. Cramer, L. G. McDonald, *Corrosion*, 48 (1992) 1009.
 15. M. Faller, D. Reiss, *Mater. Corros.*, 56 (2005) 244.
 16. A. U. Leuenberger-Minger, M. Faller and P. Richner, *Mater. Corros.*, 53 (2002) 157.
 17. J. Hedberg, N. Le Bozec, I. Odnevall Wallinder, *Mater. Corros.*, 64 (2013) 300.
 18. E. Meraz, L. Veleva, M. Acosta, *Rev. Metal. (Madrid, Spain)*, 43 (2007) 85.
 19. P. Quintana, L. Veleva, W. Cauich, R. Pomes, J.L. Peña, *Appl. Surf. Sci.*, 99 (1996) 325.
 20. L. Veleva, M. Acosta, E. Meraz, *Corros. Sci.*, 51 (2009) 2055.
 21. L. Veleva, E. Meraz, M. Acosta, *Corros. Eng., Sci. Technol.*, 45 (2010) 76.
 22. Siemens, DIFFRAC, AT-V.3.2., SOCABIM, Germany, (1994).
 23. JCPDS, International Center for Diffraction Data, Newtown Square, PA, (1993).
 24. ASTM D1141-98, *Standard Practice for the Preparation of Substitute Ocean Water*, West Conshohocken, PA: ASTM International, (2008).
 25. J. Izquierdo, L. Nagy, Á. Varga, J. J. Santana, G. Nagy, R. M. Souto, *Electrochim. Acta*, 56 (2011) 8846.
 26. J. Izquierdo, L. Nagy, I. Bitter, R. M. Souto, G. Nagy, *Electrochim Acta*, 87 (2013) 283.
 27. B. M. Fernández-Pérez, J. Izquierdo, S. González, R. M. Souto, *J. Solid State Electrochem.*, 18 (2014) 2983.
 28. A. Saleh, U. M. Anees, *Effect of Seawater Level on Corrosion. Behavior of different alloys*, Jeddah: Saline Water Conversion Corporation (SWCC), (2005).
 29. D. C. Harris, *Quantitative Chemical Analysis*, Freeman and Company, New York (2010).
 30. C. Karlén, I. Odnevall Wallinder, D. Heijerick, C. Leygraf, C. R. Janssen, *Sci. Total Environ.*, 277 (2001) 169.
 31. R. M. Souto, Y. González-García, D. Battistel, S. Daniele, *Chem. - Eur. J.*, 17 (2012) 230.
 32. R. M. Souto, Y. González-García, A. C. Bastos, A. M. Simões, *Corros. Sci.*, 49 (2007) 4568.